

Support Information

Molten salt-mediated cyano group augmentation and morphology modulation in carbon nitride for boosting photocatalytic activity

Jiahao Song^a, Heng Li^{a}, Zihao Yuan^a, Enze Hu^a, Hongfei Bao^a, Dongdong Zhang^a, Huilin Hou^a,*

Weiyu Yang^a, Hongli Yang^{a} and Xiaoqiang Zhan^{a*}*

^aInstitute of Micro/Nano Materials and Devices, Ningbo University of Technology, Ningbo, 315211, P.

R. China

*Corresponding authors. E-mails: liheng2043@outlook.com (H. Li), cumtmaterial@163.com (H. Yang) and zhanxiaoqiang777@163.com (X. Zhan)

Tel: +86-574-87080966, Fax: +86-574-87081221.

Computer methods

All density functional theory calculations were carried out with the Vienna ab initio simulation package (VASP) version 6.2.1. The exchange-correlation energy was described using the Perdew-Burke-Ernzerhof (PBE) functional within the generalized gradient approximation framework. The interaction between valence electrons and ionic cores was treated by the projector augmented-wave (PAW) approach. A kinetic energy cutoff of 500 eV was adopted for the plane-wave basis set. Structural relaxations were considered converged when the total energy change between successive electronic steps was below 1×10^{-5} eV and the residual force on each atom was less than 0.02 eV/Å. To account for long-range dispersion effects, Grimme's D3 correction was included in all calculations. The adsorption energy was evaluated according to the following expression:

$$E_{\text{ads}} = E_{\text{tot}} - (E_{\text{sub}} + E_{\text{mol}})$$

where E_{tot} is the total energy of the adsorbate-substrate complex, E_{sub} is the energy of the isolated substrate, and E_{mol} is the energy of the isolated adsorbate.

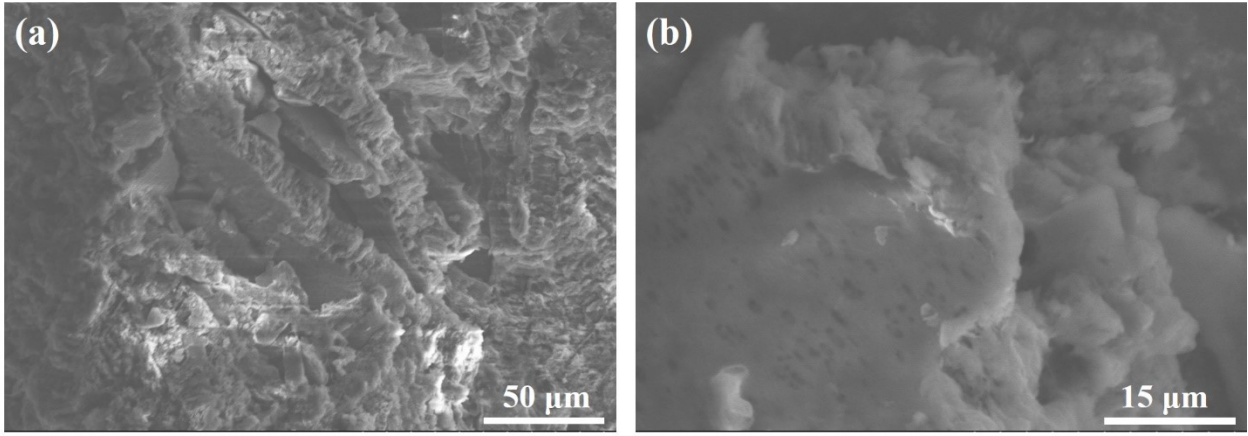


Fig. S1 SEM images of TCN

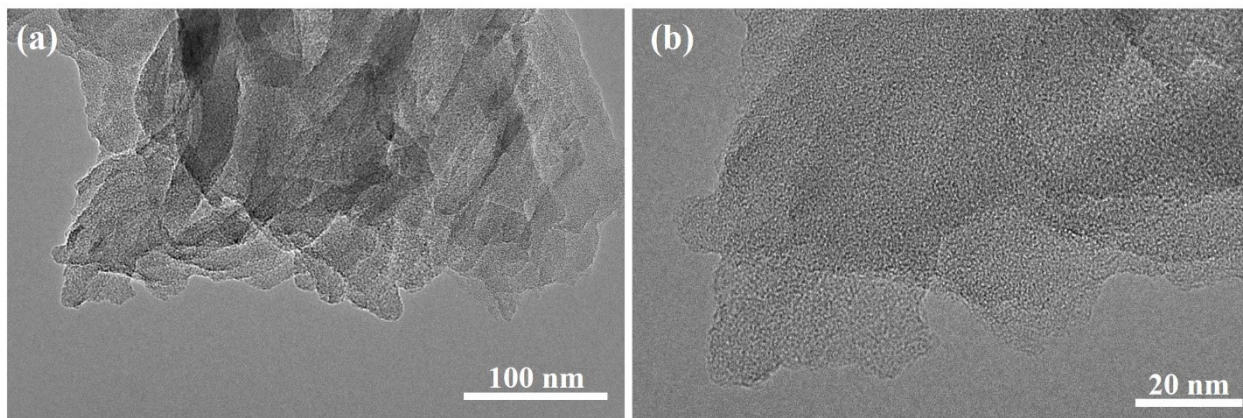


Fig. S2 (a) TEM images and (b) HRTEM images of TCN

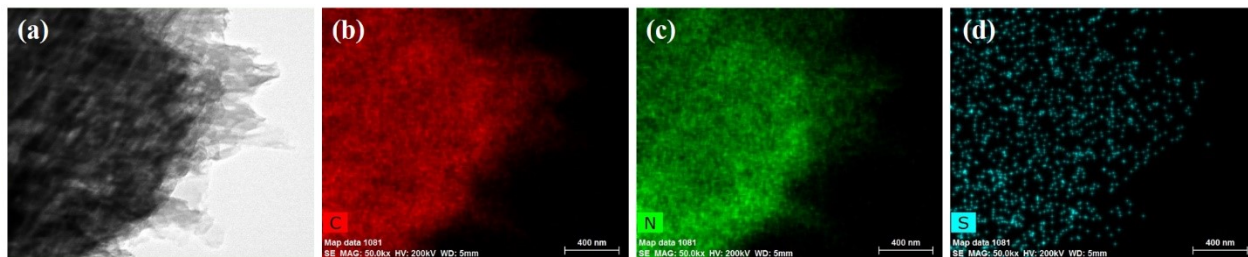


Fig. S3 TEM-EDS elemental maps of TCN

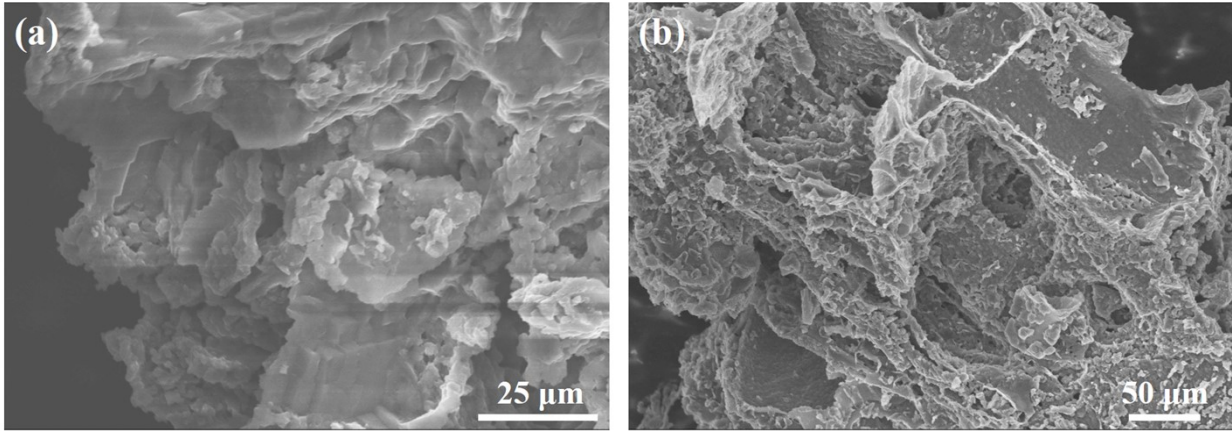


Fig. S4 SEM images of T-CN-K

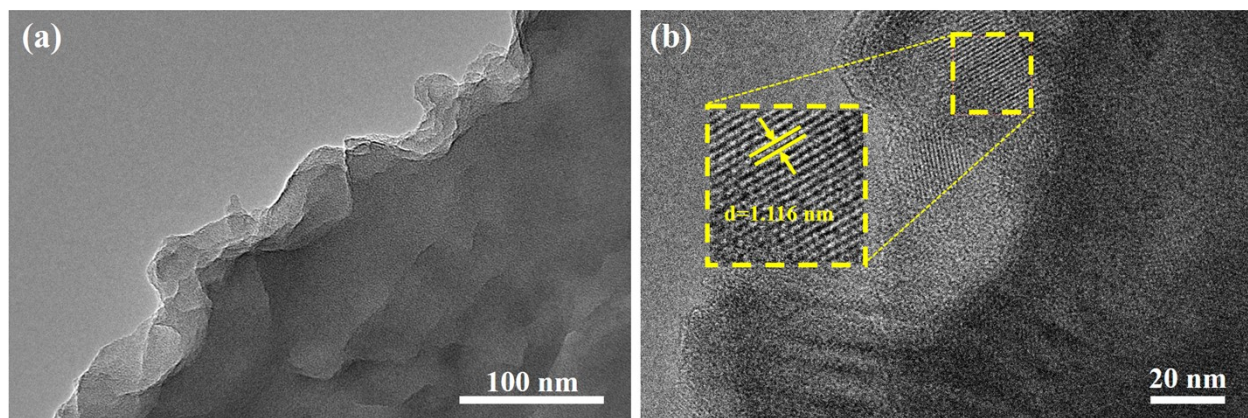


Fig. S5 TEM images and HRTEM images of T-CN-K

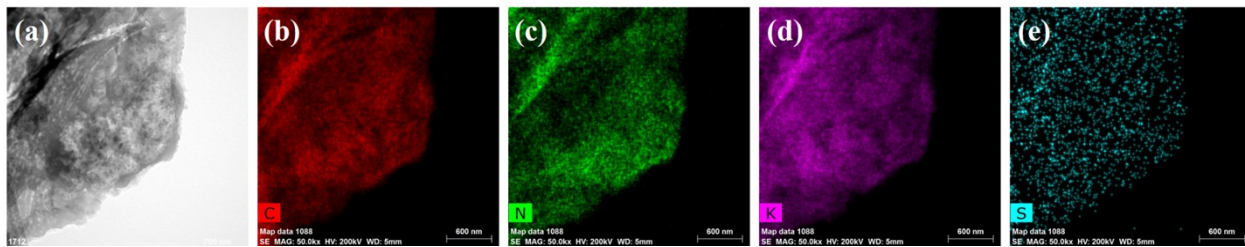


Fig. S6 TEM-EDS elemental maps of T-CN-K

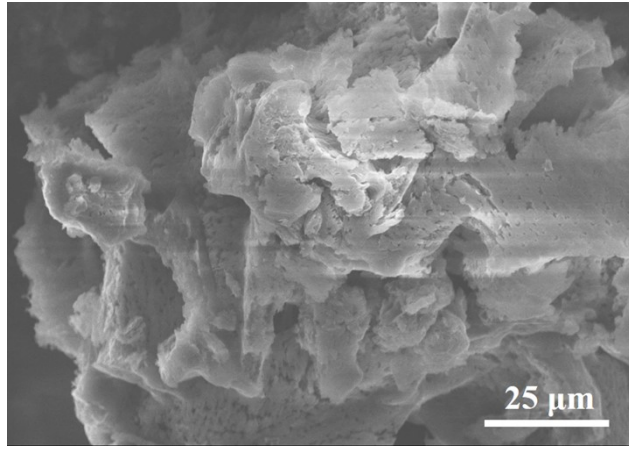


Fig. S7 SEM images of U1T5-CN

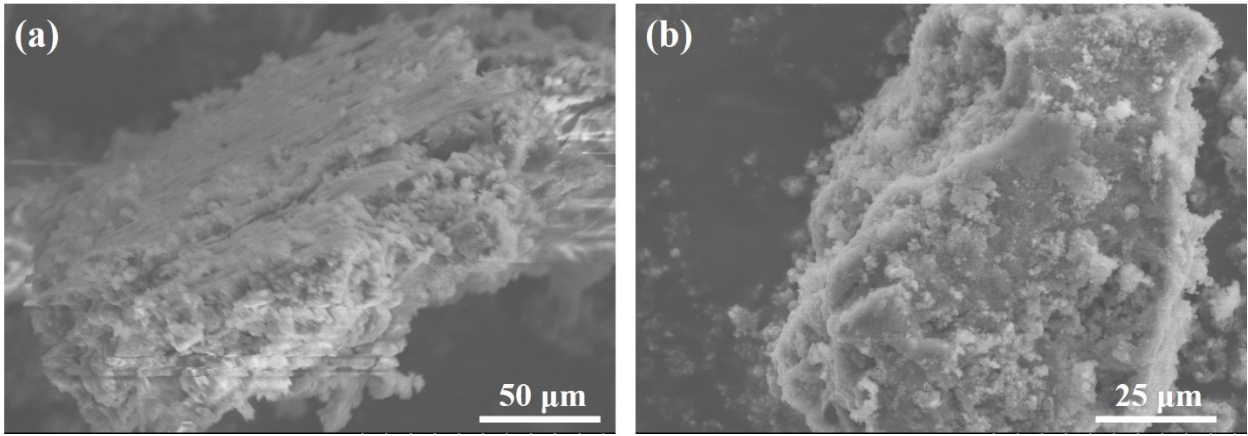


Fig. S8 SEM images of U1T5-CN-K

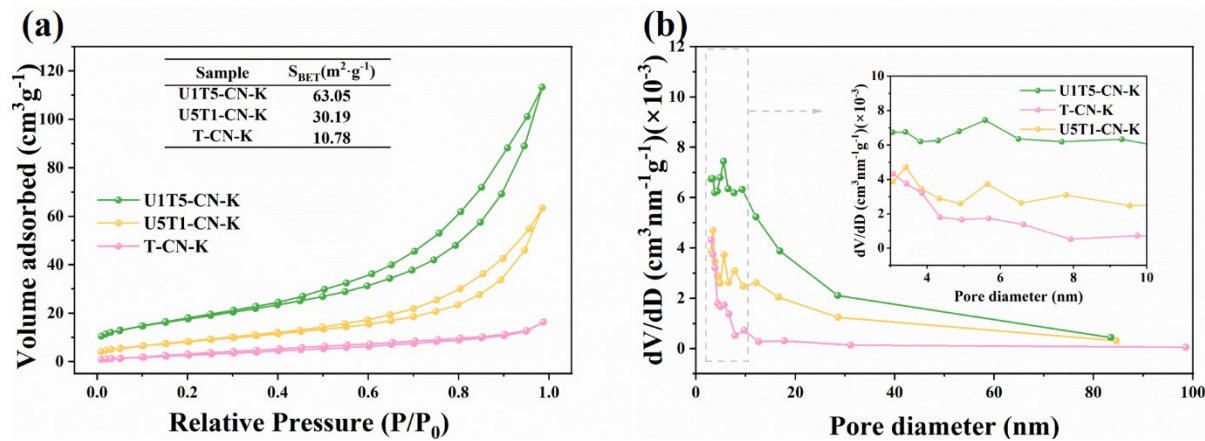


Fig. S9 (a) N_2 adsorption-desorption isotherms and (b) pore size distribution of U1T5-CN-K, U5T1-CN-K and T-CN-K

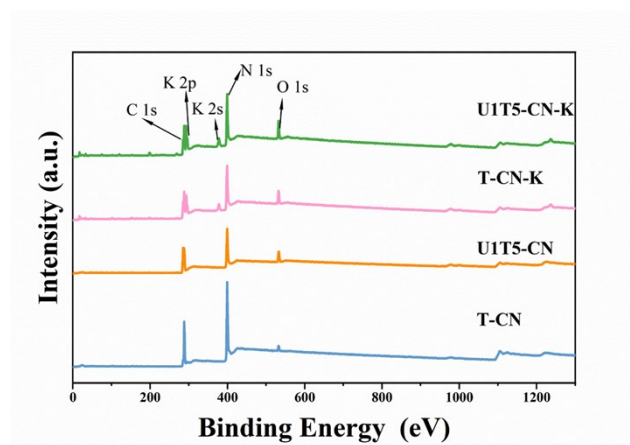


Fig. S10 XPS survey spectra of the prepared samples.

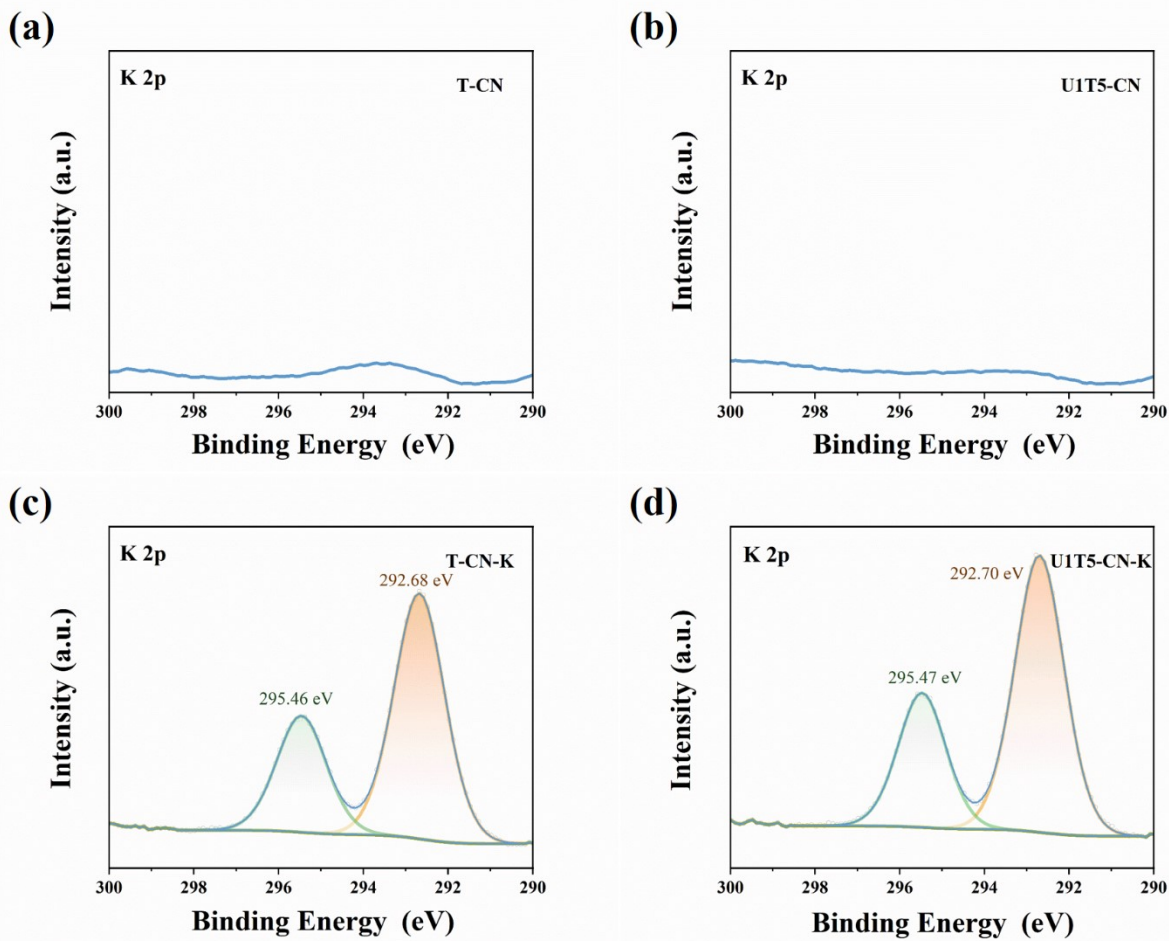


Fig. S11 High-resolution XPS spectra of K 2p of (a) T-CN, (b) U1T5-CN, (c) T-CN-K and (d) U1T5-CN-K.

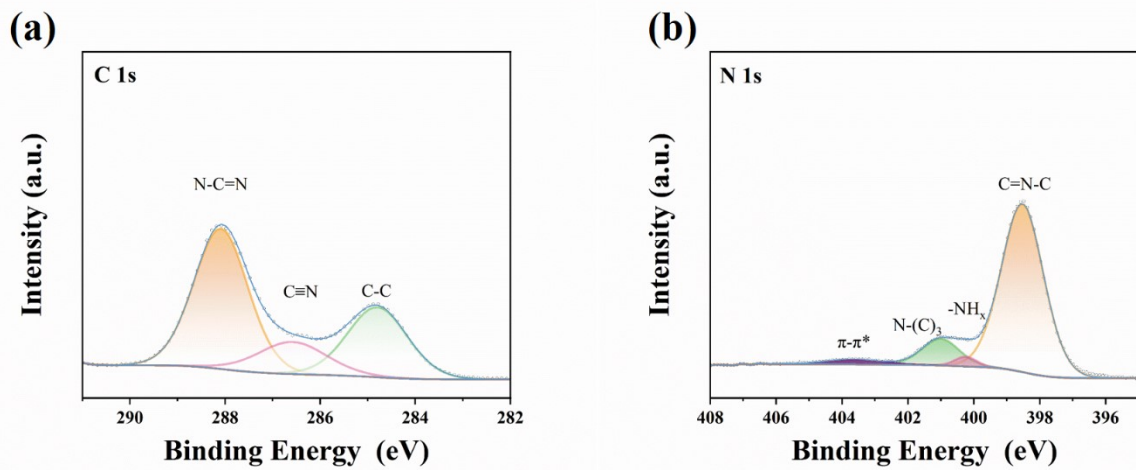


Fig. S12 High-resolution XPS spectra of (a) C 1s and (b) N1s of U5T1-CN-K.

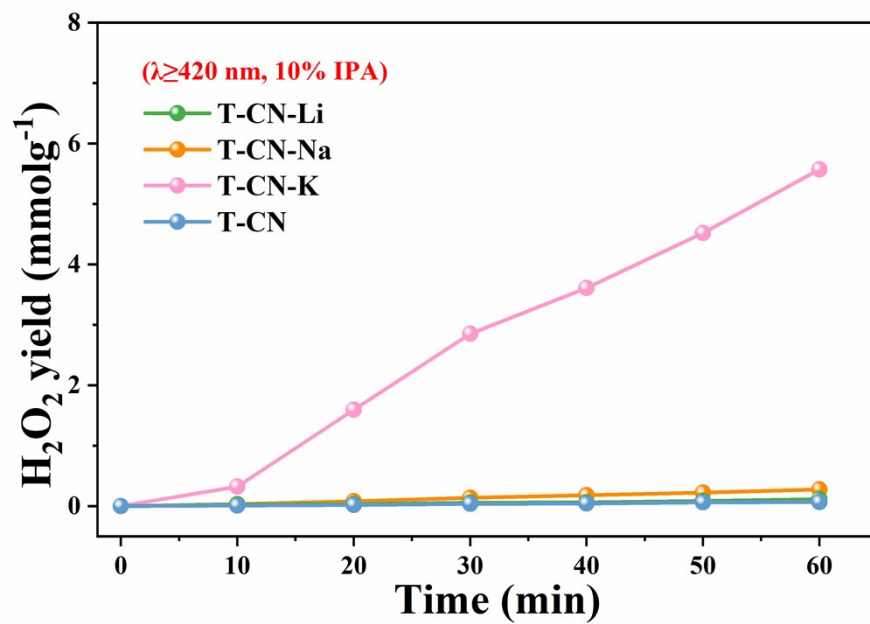


Fig. S13 Photocatalytic yield of H_2O_2 on photocatalysts doped with different alkali-metal elements

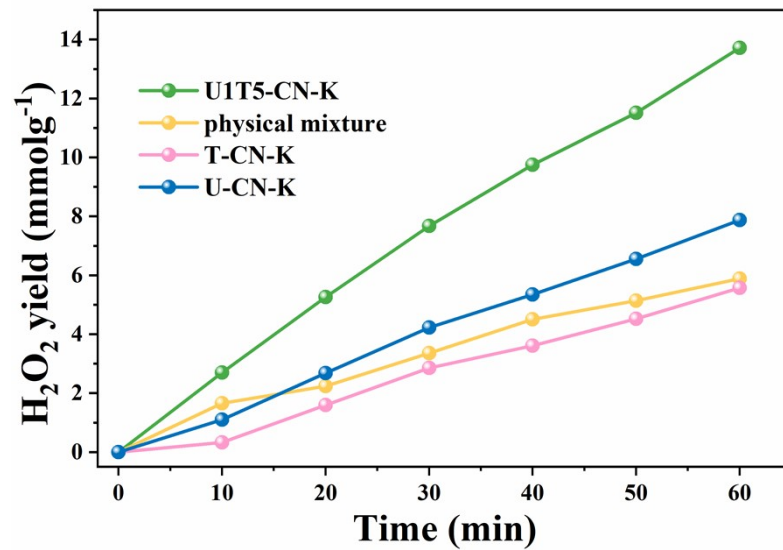


Fig. S14 Photocatalytic yield of H₂O₂ of U1T5-CN-K and physical mixture of U-CN-K and T-CN-K (mass ratio = 1:5).

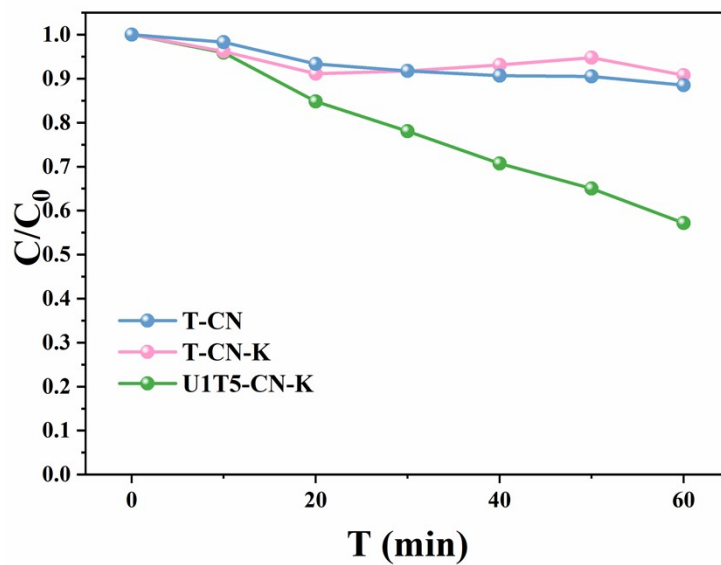


Fig. S15 Photocatalytic decomposition of H₂O₂ on different samples under visible light irradiation

($\lambda \geq 420$ nm, 1 mM H₂O₂ solution, 10 mg of catalyst, 25 °C)

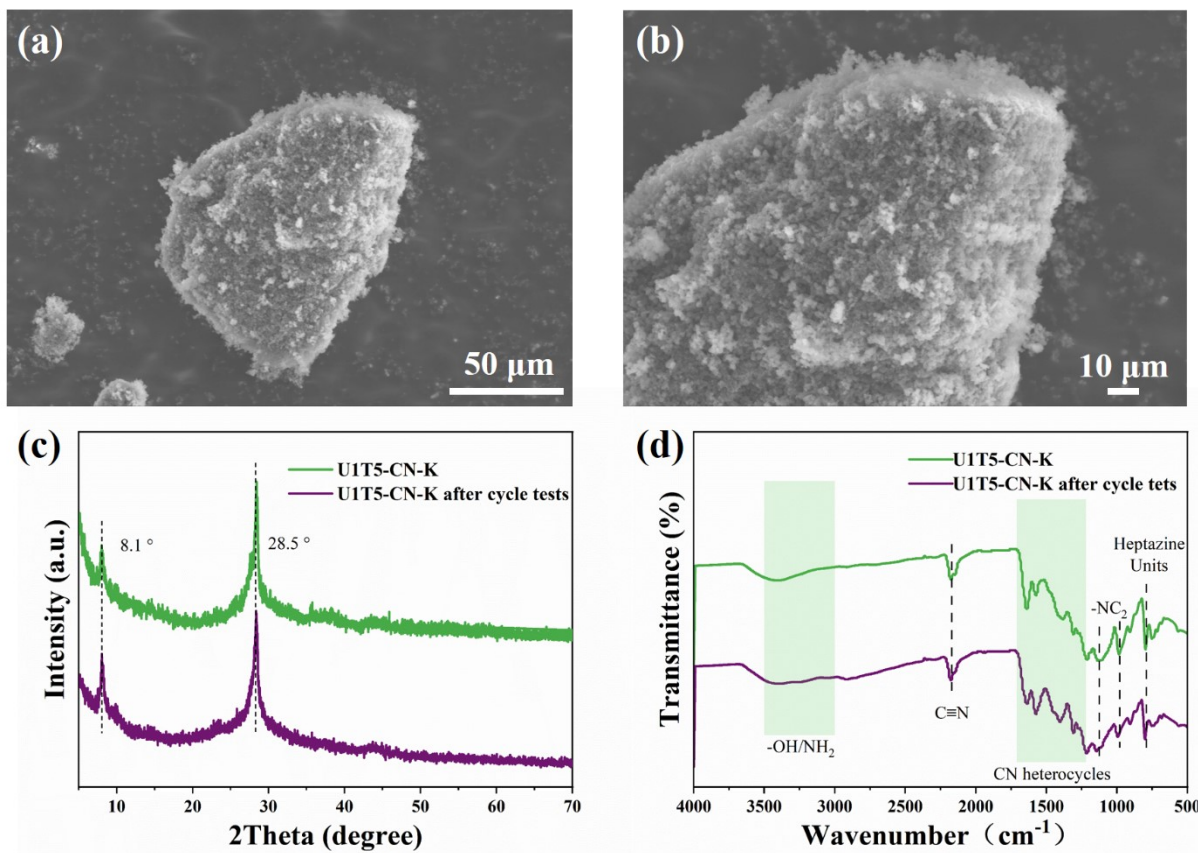


Fig. S16 (a-b) SEM images, (c) XRD patterns, and (d) FT-IR spectra of UIT5-CN-K after stability tests.

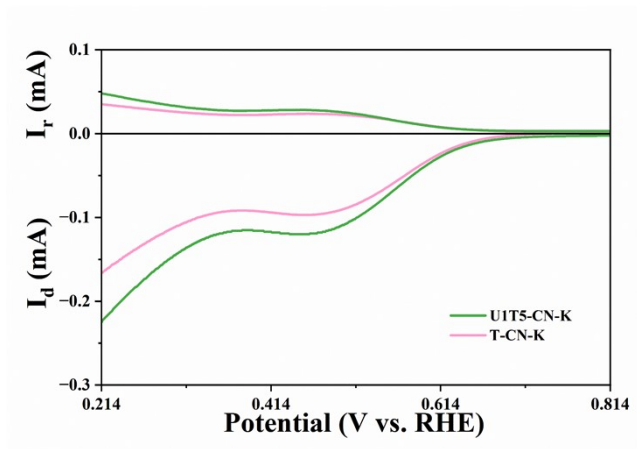


Fig. S17 RRDE polarization curves over T-CN-K and U1T5-CN-K

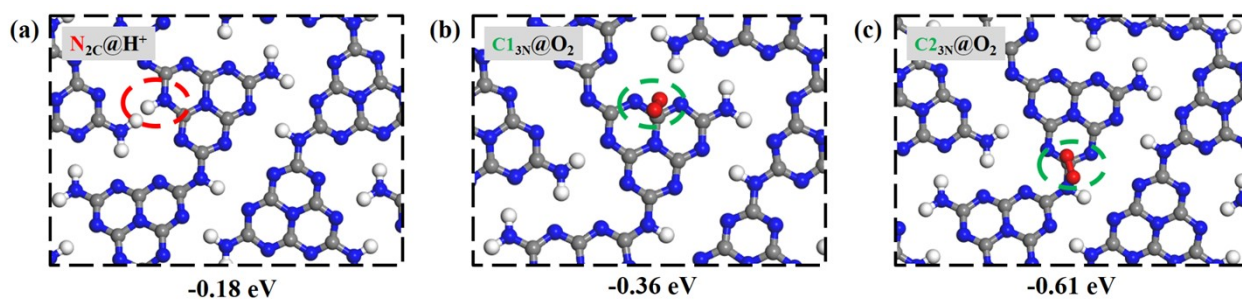


Fig. S18 The position of H^+ (red) and O_2 (green) adsorption and the corresponding energy on T-CN.

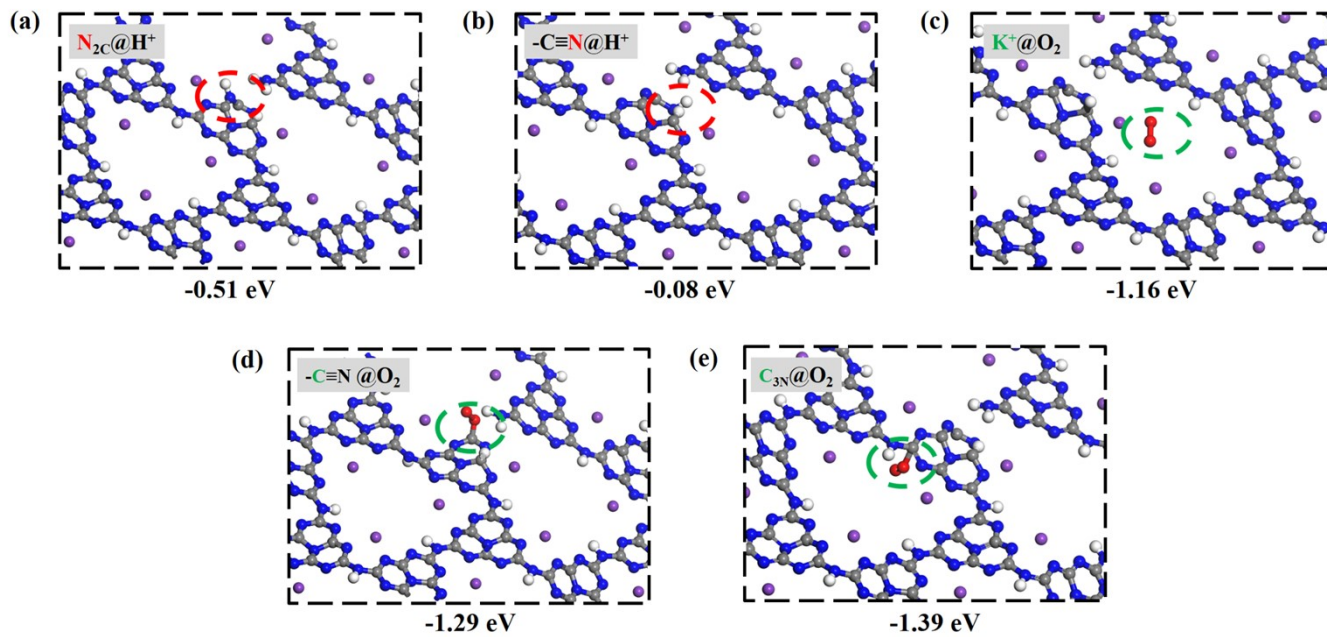


Fig. S19 The position of H^+ (red) and O_2 (green) adsorption and the corresponding energy on UIT5-CN-K.

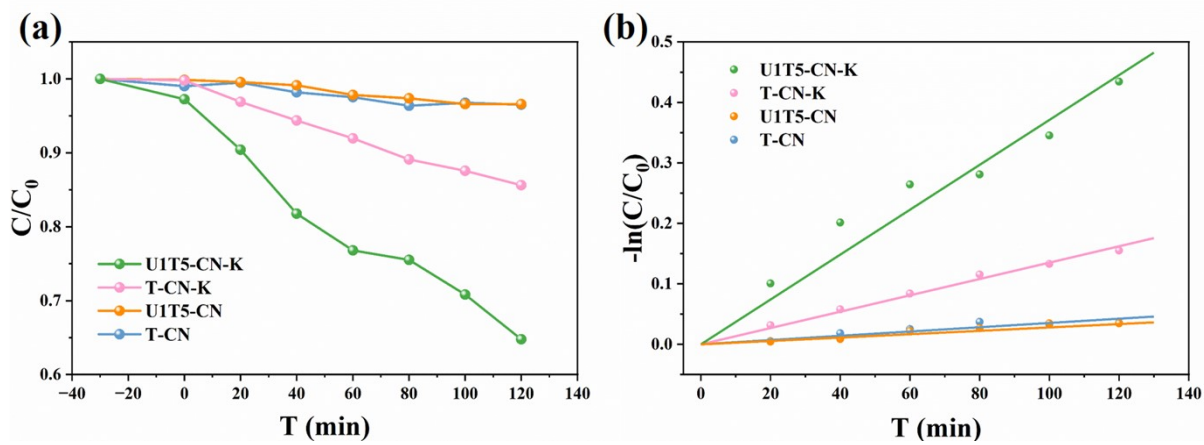


Fig. S20 (a) The degradation activity and (b) the corresponding first-order kinetic curves of the catalysts

Table S1. chemicals and reagents

Chemical	Grade	Company
Thiourea	AR, 99.0%	Shanghai Aladdin Biochemical Technology Co., Ltd.
Urea	AR	Sinopharm Chemical Reagent Co., Ltd.
Potassium chloride	AR	Sinopharm Chemical Reagent Co., Ltd.
Anhydrous ethanol	AR, 99.7%	Shanghai Macklin Biochemical Co., Ltd.
Nafion	5 wt%	Shanghai Aladdin Biochemical Technology Co., Ltd.
Potassium iodide	AR, 99.0%	Shanghai Aladdin Biochemical Technology Co., Ltd.
Potassium biphthalate	AR, 99.8%	Shanghai Macklin Biochemical Co., Ltd.
Deionized water	18.2 M Ω cm	Self-made

Table S2. Calculated distance of (100) plane and (002) plane.

Photocatalysts	(100)		(002)	
	2θ	Cal. Distance (nm)	2θ	Cal. Distance (nm)
T-CN	13.3 °	0.665	27.6 °	0.323
U1T5-CN	13.3 °	0.665	27.9 °	0.321
T-CN-K	8.1 °	1.091	28.5 °	0.313
U1T5-CN-K	8.1 °	1.091	28.5 °	0.313

Table S3. Element contents of T-CN, U1T5-CN, T-CN-K and U1T5-CN-K determined by XPS.

Samples	C	N	O	K
T-CN	43.71	53.36	2.94	-
U1T5-CN	58.52	34.35	7.12	-
T-CN-K	42.91	41.74	8.62	6.73
U1T5-CN-K	37.94	45.4	4.03	12.63

Table S4. Relative ratios of C-C, -C≡N/C-NH_x and N-C=N of the prepared photocatalysts determined by C 1s XPS spectra.

Photocatalysts	Deconvoluted C 1s (at. %)		
	C-C	-C≡N/C-NH _x	N-C=N
T-CN	13.54	3.25	83.21
U1T5-CN	49.38	5.70	44.92
T-CN-K	39.09	7.98	52.93
U1T5-CN-K	18.26	20.35	61.39
U5T1-CN-K	30.00	15.65	54.36

Table S5. Relative ratios of C=N-C, -NH_x and N-(C)³ of the prepared photocatalysts determined by N 1s XPS spectra.

Photocatalysts	Deconvoluted N 1s (at. %)		
	C=N-C	-NH _x	N-(C) ³
T-CN	76.85	12.92	10.24
U1T5-CN	75.75	13.71	10.53
T-CN-K	85.54	3.26	11.19
U1T5-CN-K	85.59	3.00	11.41
U5T1-CN-K	85.46	3.15	11.40

Table S6. H₂O₂ production performance of the catalysts with different ratios of urea/thiourea.

Photocatalysts	ratios of urea/thiourea	H₂O₂ Production rate (mmol g⁻¹ h⁻¹)
U1T5-CN-K	1:5	13.71
U3T3-CN-K	3:3	10.78
U5T1-CN-K	5:1	9.68

Table S7. H₂O₂ production performance of the catalysts and the enhancement ratio compared to UIT5-CN-K.

Photocatalysts	H₂O₂ Production rate (mmolg⁻¹h⁻¹)	Ratio (UIT5-CN-K vs sample)
T-CN	0.068	201.6
UIT5-CN	0.113	121.3
T-CN-K	5.57	2.5
UIT5-CN-K	13.71	1.0

Table S8. Wavelength-dependent AQY for U1T5-CN-K in photocatalytic H₂O₂ generation.

Wavelength	H₂O₂	Irradiation	Irradiation area	Irradiation time	AQY(%)
h	yield	intensity	(m²)	(s)	
(nm)	(μmol)	(Wm⁻²)			
400	155.9	531.9	3.32×10 ⁻³	3600	1.47
420	164.3	565.8	3.32×10 ⁻³	3600	1.39
450	97.6	651.0	3.32×10 ⁻³	3600	0.67
475	10.1	667.7	3.32×10 ⁻³	3600	0.064
500	7.75	605.4	3.32×10 ⁻³	3600	0.051

Table S9. Comparison of the performance of photocatalytic H₂O₂ production in the reported literature.

Photocatalyst	Reaction solution	Catalyst dose	Light source	H ₂ O ₂ yield	Ref.
UIT5-CN-K	isopropanol (10%)	0.2 g L ⁻¹	300W Xe lamp ($\lambda \geq 420$ nm)	13.71 mmol g ⁻¹ h ⁻¹	this work
ACNN	isopropanol (10%)	0.5 g L ⁻¹	300W Xe lamp ($\lambda \geq 420$ nm)	10.2 mmol g ⁻¹ h ⁻¹	1
KCN-4	isopropanol (10%)	0.2 g L ⁻¹	300W Xe lamp ($\lambda \geq 420$ nm)	6.12 mmol g ⁻¹ h ⁻¹	2
P, N-C@CNHS	isopropanol (10%)	0.5 g L ⁻¹	300W Xe lamp ($\lambda \geq 420$ nm)	4.57 mmol g ⁻¹ h ⁻¹	3
Ni-UPGCN	isopropanol (10%)	2.0 g L ⁻¹	300W Xe lamp ($\lambda \geq 420$ nm)	4.12 mmol g ⁻¹ h ⁻¹	4
Br-PCN	isopropanol (10%)	1.0 g L ⁻¹	300W Xe lamp ($\lambda \geq 420$ nm)	3.98 mmol g ⁻¹ h ⁻¹	5
MCN-200B-LiK	ethanol (10%)	1.0 g L ⁻¹	300W Xe lamp ($\lambda \geq 420$ nm)	2.42 mmol g ⁻¹ h ⁻¹	6
B-CN/P-CN	ethanol (10%)	0.4 g L ⁻¹	300W Xe lamp ($\lambda \geq 420$ nm)	2.20 mmol g ⁻¹ h ⁻¹	7
CACN	ethanol (10%)	0.4 g L ⁻¹	300 W xenon lamp (AM 1.5)	1.60 mmol g ⁻¹ h ⁻¹	8
KCN-6	ethanol (10%)	0.5 g L ⁻¹	300W Xe lamp ($\lambda \geq 420$ nm)	0.82 mmol g ⁻¹ h ⁻¹	9
B-g-C ₃ N ₄ -20	isopropanol (10%)	1.0 g L ⁻¹	300W Xe lamp ($\lambda \geq 420$ nm)	0.42 mmol g ⁻¹ h ⁻¹	10

Table S10. H₂O₂ production performance of UIT5-CN-K in the presence of various trapping agents

Gents	H₂O₂ production rate (mmol g⁻¹ h⁻¹)	Ratio (%) to original performance
N ₂	0.540	3.9%
AgNO ₃	0.268	2.0%
Nitroblue tetrazolium chloride (NBT)	2.404	17.5%
Pure water	0.865	6.30%

Table S11. The TH (170 mg L⁻¹) degradation performance of the prepared photocatalysts

Catalyst	Degradation rate (%)	The amount of degraded TH	k value
		(mg L⁻¹)	(min⁻¹)
T-CN	3.50	5.95	0.0356
U1T5-CN	3.42	5.81	0.0348
T-CN-K	14.38	24.45	0.1553
U1T5-CN-K	35.22	59.87	0.4342

References

1. S. Wu, H. Yu, S. Chen and X. Quan, *ACS Catal.*, 2020, 10, 14380-14389.
2. Y. Wang, X. Shi, W. Li, Y. Wang and W. Yao, *ACS Omega*, 2024, 9, 41043-41052.
3. X. Dang, X. Cui, H. Zhang, X. Chen and H. Zhao, *ACS Sustainable Chem. Eng.*, 2023, 11, 13096-13107.
4. X. Zhou, K. Wang, Y. Wang, Y. Cao, J. Wang, H. Hu, G. Yang, J. Hou, P. Ma, C. Gao, C. Ban, Y. Duan, Z. Wei, X. Zhang, C. Wang and K. Zheng, *Langmuir*, 2024, 40, 11251-11262.
5. A. Gupta, T. Bhoyar, B. M. Abraham, D. J. Kim, K. S. Pasupuleti, S. S. Umare, D. Vidyasagar and A. Gedanken, *ACS Appl. Mater. Interfaces*, 2023, 15, 18898-18906.
6. C. Xu, W. Zheng, X. Liu, J. Li, W. Lai, X. Liang, Y. Chen, D. Fan and H. Pan, *J. Mater. Chem. A*, 2026,
7. S. Khan, M. A. Qaiser, W. A. Qureshi, Y. Xu, J. Li, H. Li, L. Sun, S. N.-u.-Z. Haider, B. Zhu, L. Wang, W. Wang and Q. Liu, *ACS Appl. Mater. Interfaces*, 2025, 17, 6249-6259.
8. Q. Xu, J. Wu, Y. Qian, X. Chen, Y. Han, X. Zeng, B. Qiu and Q. Zhu, *ACS Appl. Mater. Interfaces*, 2024, 16, 784-794.
9. X. Tantai, Q. Zhou, L. Shi, M. Wu, P. Sun and X. Dong, *ACS Appl. Nano Mater.*, 2025, 8, 19001-19011.
10. T. Wang, L. Zhang, L. Sun, J. Zhao, Y. Wang, Z. Qu and Y. Wang, *ACS Appl. Nano Mater.*, 2025, 8, 16533-16539.